First Steps in the Phytochrome Phototransformation: A Comparative Femtosecond Study on the Forward (Pr → Pfr) and Back Reaction (Pfr → Pr)†

Mark Bischoff,‡ Gudrun Hermann,*,§ Sabine Rentsch,‡ and Dietmar Strehlow§

Institute for Optics and Quantumelectronics, Friedrich-Schiller-University, Max-Wien-Platz 1, D-07743 Jena, and Department of Biochemistry and Biophysics, Friedrich-Schiller-University, Philosophenweg 12, D-07743 Jena, Germany

Received May 24, 2000; Revised Manuscript Received October 24, 2000

ABSTRACT: The primary light-induced events in the reversible Pr ⇌ Pfr phototransformation are investigated by femtosecond absorption spectroscopy using a pump−probe technique. After the selective electronic excitation of Pr and Pfr with pulses at 610 and 730 nm, respectively, the transient absorption spectra were measured as a function of the delay time and subjected to a global fit analysis. As a result of this analysis, the decay-associated spectra of the kinetic components involved in the formation of the first photoproducts in the forward and back reaction are obtained. These spectra provide a more detailed understanding of the primary stages in the light-induced transformations. In addition, the influence of the solvent viscosity on the initial reaction steps was studied. In each direction of reaction, a short-lifetime component is found to be strongly viscosity-dependent, indicating that the primary photochemistry encompasses intramolecular motions of the chromophore or its proximal amino acid side chains. H−D exchange has no significant effect on the kinetics of the initial photoprocesses. This suggests that the isomerization reaction in both directions is not accompanied by a rate-limiting proton transfer.

Phytochromes make up a class of photoreceptors in plants and cyanobacteria which absorb light in the red and far-red region of the spectrum (*1*−*3*). Light perception is mediated by two different phytochrome forms, the red light-absorbing form (Pr)[1] and the far-red light-absorbing form (Pfr). These two forms can be reversibly interconverted by the sequential absorption of red and far-red light. The molecular changes associated with the Pr and Pfr photoconversion affect signal transduction processes which result in a modification of developmental responses according to the prevailing light conditions.

The first photochemical step following the light absorption involves a *Z*,*E* isomerization of the tetrapyrrolic chromophore (*4*, *5*). The initial, fast isomerization triggers a series of thermal reactions during which a number of metastable intermediates with lifetimes in the microsecond to millisecond time domain are generated (*6*−*10*). Up to six intermediates have been identified in the forward phototransformation (from Pr to Pfr) and three intermediates in the back reaction (from Pfr to Pr). On the basis of a comparison of the spectral and kinetic properties, it seems very likely that the Pr phototransformation pathway does not share any intermediate with the Pfr photoreversion pathway.

The issue of structural changes forming the intermediate states is the central question in current studies. The consensus of FT Raman and FTIR studies using low-temperature trapping techniques is that the double-bond isomerization of the tetrapyrrolic chromophore has occurred already in the first detectable photoproducts of Pr and Pfr, viz., lumi-R and lumi-F, respectively (*11*−*15*). However, there is a gap in the understanding of the early light-induced ultrafast events leading to the formation of these first photoproducts. The elucidation of the primary events following the light absorption is of great interest because they are related to key questions such as the causes for the selectivity of the photoreaction which excludes unwanted side reactions as well as the molecular mechanism by which light energy is initially stored in the excited chromophore and subsequently used for protein conformational changes which drive the functional processes.

In the past years, picosecond and femtosecond spectroscopic techniques have been employed to gain some insight into the first steps of the phototransformation. With respect to the Pr ⇌ Pfr transformation, early experiments with picosecond time resolution indicated the presence of two excited electronic states with lifetimes in the range of 5−15 and ∼40 ps depending on the experimental conditions (*16*−*20*). These experiments further indicated the formation of a first transient reaction product, assigned to lumi-R, within tens of picoseconds. Through the use of femtosecond spectroscopy at a low repetition rate of 1 Hz, we have since established lifetimes of ∼3 and 32 ps for the two excited states where the 32 ps lifetime correlates to the rise time of the lumi-R formation (*21*). In addition, using femtosecond spectroscopy, we were also able to resolve the ultrafast light-induced events in the Pfr → Pr back reaction which appear to be considerably faster than the early events in the forward photoreaction (*22*, *23*). The decay of the initially excited state has been observed with a ∼700 fs time constant, yielding

† The financial support of this work by the Deutsche Forschungsgemeinschaft is greatly appreciated.

* To whom correspondence should be addressed: Department of Biochemistry and Biophysics, Friedrich-Schiller-University, Philosophenweg 12, D-07743 Jena, Germany. Telephone: (+3641) 949 376. Fax: (+3641) 949 352. E-mail: bgh@rz.uni-jena.de.

‡ Institute for Optics and Quantumelectronics.

§ Department of Biochemistry and Biophysics.

[1] Abbreviations: *A*, optical density; Pfr, far-red light-absorbing form of phytochrome; Pr, red light-absorbing form of phytochrome.

10.1021/bi0011734 CCC: $20.00
Published on Web 12/07/2000

another electronic state which converts with 4.5 ps into an, as yet poorly characterized, intermediate product state.

In our previous femtosecond studies, we carried out kinetic measurements at distinct probe wavelengths. In this paper, we present a more detailed analysis of the ultrafast events in the Pr → Pfr and Pfr → Pr phototransformation path which became available by measuring the transient absorption spectra over a wide spectral range of 450−850 nm at a great wealth of different delay times and estimating the decay-associated spectra of the distinct kinetic components by a global analysis approach. Furthermore, to probe the molecular nature of the ultrafast events, both the viscosity dependence of the kinetic components and the effect of deuteration on these components were examined. The experiments were carried out with native phytochrome from oat (molecular mass of 124 kDa/monomer).

EXPERIMENTAL PROCEDURES

Instrumentation and Measuring Procedure. The laser system and method of measurement employed in the time-resolved experiments have been described in detail elsewhere (*23*, *24*). Excitation of Pr was performed by femtosecond pulses at 610 nm [pulse duration of 100 fs (fwhm)] which were produced by a colliding pulse mode-locked dye laser with a four-stage dye amplifier. The repetition rate of the laser system was 15 Hz. A broadband femtosecond white light continuum (spectral range of 450−850 nm) generated in a sapphire plate was used for probing. The chirp of the white light continuum was numerically compensated to <0.2 fs/nm. The pump and probe beams were aligned parallel to each other. For the excitation of Pfr, the continuum pulses served as seed pulses for a two-stage postamplifier that produced pulses at 730 nm [pulse duration of 150 fs (fwhm)] after recompression. The probe light transmitted through the samples was detected by a CCD camera after the light had been passed through a grating polychromator. The spectral resolution of the measurements was better than 5 nm. The absorption changes were measured as the difference between the optical densities (ΔA) with and without excitation. To monitor the time evolution of the absorption changes, the probe pulse was delayed with respect to the excitation pulse by means of a variable optical delay line. By averaging over at least 50 laser shots at each delay time, statistical fluctuations of the excitation and probe pulse were compensated. All instrumentation in the pump−probe spectrometer was controlled by a computer using homemade software. The measurements were carried out at 293 K.

Each series of measurement was first run at a pump power 2 and 5 times lower than that ultimately used for data collecting to ensure the linearity of the results with power.

For a kinetic analysis, the experimentally measured data were first compensated for the probe chirp and then fitted to a sum of exponentials including a constant term by a global fit analysis (*25*). The constant term was added to simulate a long-lived component, the lifetime of which cannot be determined in the time window of the femtosecond measurements. The accuracy of the estimated kinetic constants is better than ±25%.

Preparation of Phytochrome. Native phytochrome (molecular mass of 124 kDa/monomer) was isolated from 5-day-old etiolated oat seedlings (*Avena sativa* L. cv. Adamo) as reported previously (*23*). For the time-resolved experiments, it was dissolved in a 10 mM phosphate buffer at pH 7.8. The final sample absorption was set to 0.4 at 666 nm, as measured in a quartz cell with a path length of 1 mm. Over the period of the measurements, the phytochrome sample was pumped by a peristaltic pump trough a flow cell with a path length of 2 mm. The flow rate was adjusted such that each sample volume was excited only once. In the case of the measurements with Pfr, Pr was converted to Pfr by saturating illumination with red light before the experiments.

Phytochrome solutions with 67% (v/v) glycerol were prepared by mixing phytochrome in phosphate buffer with the appropriate amount of glycerol. To eliminate air bubbles, the resulting solution was degassed by vacuum and then flushed with nitrogen.

For the preparation of deuterated Pfr, phytochrome was precipitated with ammonium sulfate (230 g/L). The pellet was then washed and resuspended with deuterated phosphate buffer. After that, the phytochrome solution was repeatedly concentrated and again diluted with deuterated phosphate buffer. During this procedure, the phytochrome was maintained as Pfr since the extent of proton−deuteron exchange is increased by the residency of phytochrome in its Pfr form (*26*).

Before and after the pump−probe experiments, the photoreversibility and integrity of the phytochrome samples were examined by UV−vis spectroscopy and SDS electrophoresis. The results obtained showed that both the spectral and the structural properties were not affected by the laser exposure.

RESULTS

Pr to Pfr Phototransformation. Figure 1a shows the absorption difference spectra obtained at several delay times after femtosecond excitation of Pr at 610 nm. Immediately after excitation, a strong negative band occurs in the region of the Pr ground-state absorption which is accompanied by weak positive absorption changes at either side. In addition, a weak negative band is discernible in the far-red region (λ > 725 nm) where the Pr absorption is negligible. On the basis of our previous work, these spectral features are due to photobleaching of Pr, excited-state absorptions, and stimulated emission of Pr (*21*). At longer delay times, the spectra exhibit a photobleaching band and a small positive absorption band around 690 nm that persists for times well beyond the 500 ps time window accessible to our femtosecond measurements. These spectra obviously arise from the absorption of a comparatively long-lived photointermediate.

For a kinetic analysis, the time-dependent absorption changes were fitted to a sum of exponential functions using a global fit approach. The best fit was obtained when a sum of three exponentials and a constant term was used in the analysis. The constant term was added to simulate the long-lived residual absorption in the transient spectra, the lifetime of which cannot be determined under the femtosecond time resolution. The lifetimes estimated for the three exponential components are 360 fs (τ_1), 1.8 ps (τ_2), and 34 ps (τ_3). Figure 1b shows the amplitudes (a_i) of these components plotted versus probe wavelength (decay-associated spectra).

The 360 fs spectrum exhibits two positive bands at around 660 and >720 nm, both reflecting most likely the decay of excited-state absorptions. Furthermore, the spectrum reveals

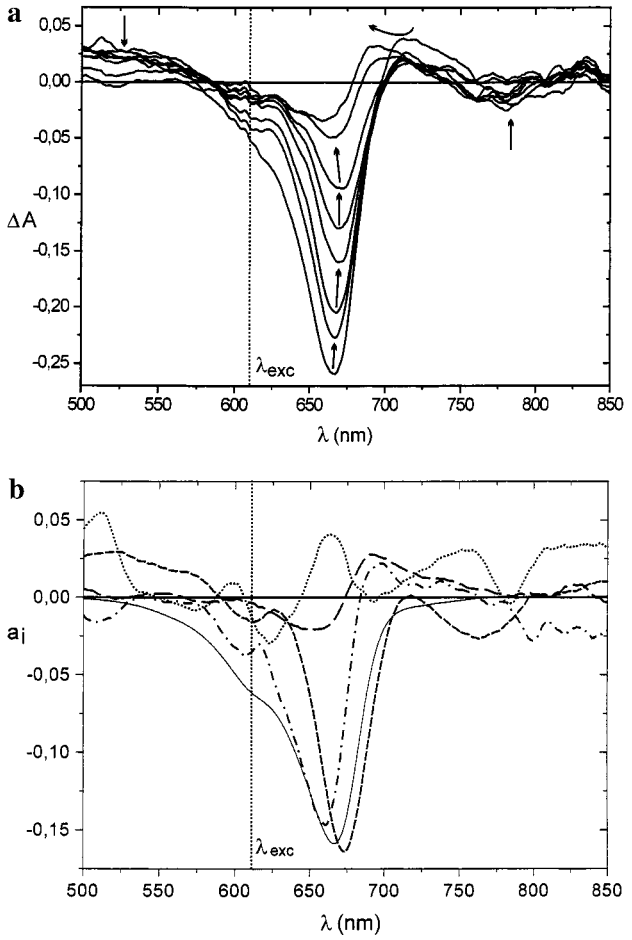

FIGURE 1: (a) Absorption difference spectra [$\Delta A(\lambda)$] recorded after excitation of Pr with 100 fs pulses at 610 nm. Eight spectra corresponding to delay times of 0.3 ps (bottom) and 1.0, 2.0, 5.0, 10, 20, 50, and 100 ps (top) are shown. (b) Amplitude spectra [$a_i(\lambda)$] of the individual kinetic components in the Pr → Pfr transformation estimated from the global fit analysis in comparison with the negative static absorption spectrum of Pr. The spectra refer to the 360 fs component (•••), the 1.8 ps component (−•−), the 34 ps component (- - -), the long-lived component (− − −), and the negative static absorption spectrum of Pr (—).

the Stokes and anti-Stokes Raman peaks of the aqueous buffer at around 770 and 510 nm (see ref *27*). In the 1.8 ps spectrum, the negative band looks similar to the inverted stationary absorption band of Pr. The negative minimum is only slightly blue-shifted from the absorption maximum due to the positive amplitudes in the region of the red excited-state absorption. The 34 ps spectrum exhibits positive amplitudes in the region of the blue excited-state absorption and negative amplitudes where the ground-state bleaching is observed. The negative band is slightly red-shifted with respect to the Pr ground-state absorption and contains a broad negative contribution in the spectral region of the stimulated emission. Altogether, the spectral shape and position of the negative band are closely related to the inverted stationary fluorescence spectrum of Pr. The spectrum of the long-lived component exhibits a negative band that matches the Pr photobleaching band and a well-developed positive band with a maximum at ~690 nm. The amplitude spectrum agrees quite well with the difference spectrum between Pr and lumi-R (Figure 2) as it is obtained from time-resolved measurements on the nanosecond time scale (*7*, *10*, *19*, *28*).

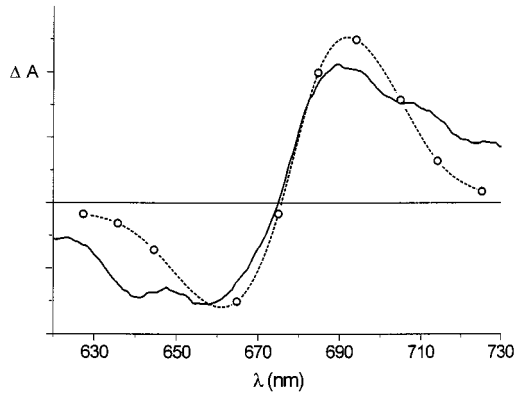

FIGURE 2: Comparison of the amplitude spectrum for the long-lived component τ_4 (—) in the Pr → Pfr transformation with the difference spectrum (- - -) between lumi-R and Pr measured in nanosecond laser flash studies (*27*).

Table 1: Kinetic Constants Estimated for the Primary Processes in the Pr → Pfr and Pfr → Pr Phototransformation[a]

	aqueous buffer	67% glycerol/buffer mixture	deuterated phytochrome
Pr → Pfr			
τ_1 (ps)	0.36	0.62	0.38[b]
τ_2 (ps)	1.8	3.6	2.3
τ_3 (ps)	34	39	31
Pfr → Pr			
τ_1 (ps)	0.56	0.99	0.68
τ_2 (ps)	3.8	4.0	4.0

[a] For the kinetic analysis, a sum of exponential functions including a constant term which accounts for the formation of a comparatively long-living intermediate was used as a fit function. The kinetic constants were obtained from a global analysis. [b] The kinetic constants determined for deuterated Pr are included in the table to complete the picture. The data confirm results of earlier studies demonstrating that the primary processes in the Pr → Pfr transformation are not subject to a kinetic isotope effect (*15*, *16*, *29*).

To probe possible molecular motions of the chromophore and/or amino acid side chains in the course of the primary photoprocesses, these processes were examined in a solvent with increased viscosity. A 67% glycerol/buffer mixture was used as such a solvent. Table 1 shows the time constants estimated for the kinetic components in the glycerol/buffer mixture and compares these values with those in the aqueous buffer. As is evident, the two fastest time constants, τ_1 and τ_2, are significantly lengthened in the more viscous medium, whereas the slower time constant, τ_3, is only slightly affected. Figure 3 gives in addition the amplitude spectra obtained in the glycerol buffer. With respect to their spectral shape and position, they do not differ from the spectra in the aqueous buffer, indicating that the spectroscopic and photochemical properties of native Pr are retained in the glycerol/buffer mixture.

Pfr to Pr Phototransformation. Figure 4a depicts the absorption difference spectra observed for several pump−probe delay times after femtosecond excitation of Pfr at 730 nm. The spectra are characterized by the prompt appearance of a negative band at the spectral position of the steady-state absorption, implying that this band is mostly due to the bleaching of the initial Pfr absorption. Concurrent with bleaching, positive absorption bands are discernible on the red and blue sides of the ground-state bleach. They are probably related to excited-state absorptions. At longer delay

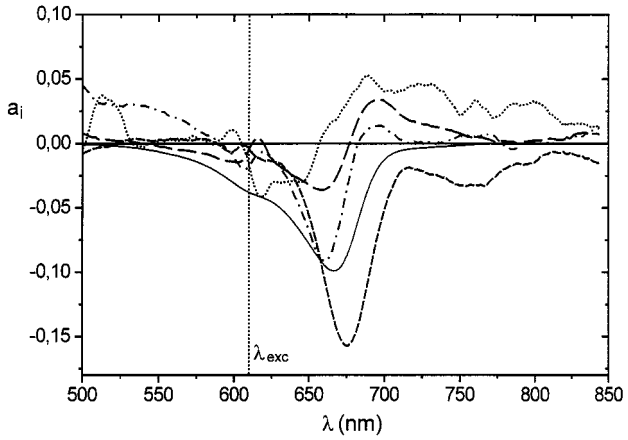

FIGURE 3: Amplitude spectra [$a_i(\lambda)$] of the individual kinetic components in the Pr → Pfr transformation estimated in a 67% glycerol/buffer mixture. The spectra refer to the 620 fs component (•••), the 3.6 ps component (—•—), the 39 ps component (- - -), the long-lived component (— — —), and the negative static absorption spectrum of Pr (—).

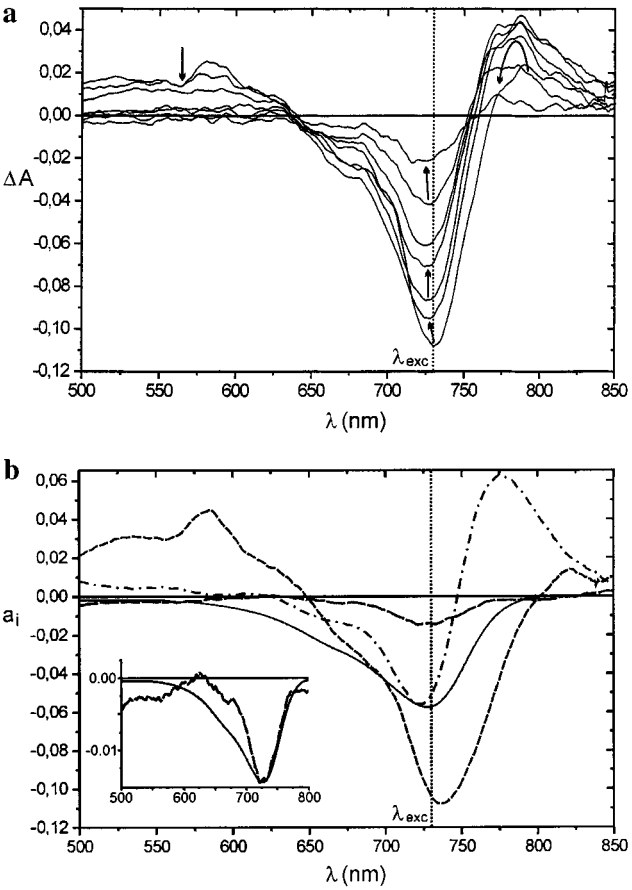

FIGURE 4: (a) Absorption difference spectra [$\Delta A(\lambda)$] recorded after excitation of Pfr with 150 fs pulses at 730 nm. Seven spectra corresponding to delay times of 0.5 ps (bottom) and 0.8, 1.0, 1.5, 2.0, 4.0, and 8.0 ps (top) are shown. (b) Amplitude spectra [$a_i(\lambda)$] of the individual kinetic components in the Pfr → Pr transformation obtained from the global fit analysis in comparison with the negative static absorption spectrum of Pfr. The spectra refer to the 560 fs component (- - -), the 3.8 ps component (—•—), the long-lived component (— — —), and the negative static absorption spectrum of Pfr (—). The inset shows a comparison between the amplitude spectrum of the long-lived component (— — —) and the negative static absorption spectrum of Pfr (—).

times, the ground-state depletion recovers more slowly than the excited-state absorptions decay, indicating that the excited

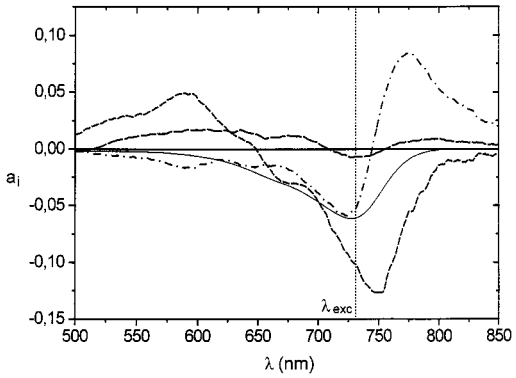

FIGURE 5: Amplitude spectra [$a_i(\lambda)$] of the individual kinetic components in the Pfr → Pr transformation estimated in a 67% glycerol/buffer mixture. The spectra refer to the 990 fs component (- - -), the 4.0 ps component (—•—), the long-lived component (— — —), and the negative static absorption spectrum of Pfr (—).

state not only decays to the ground state directly but also undergoes relaxation toward an intermediate state.

A kinetic analysis using the global fit routine reveals that two exponential components with lifetimes of 560 fs (τ_1) and 3.8 ps (τ_2), in addition to a long-lived component (τ_3), give rise to the observed absorption changes (Table 1). Figure 4b shows the amplitude spectra for each of the kinetic components. The spectrum of the 560 fs component has a strong negative band in the spectral region of the Pfr ground-state absorption and broad positive contributions flanking the shortwave side of the negative band. The negative band is slightly shifted to the red from the ground-state absorption spectrum and obviously contains negative contributions in the red wing due to stimulated emission. The 3.8 ps component also has negative amplitudes in the region of the ground-state absorption and strong positive amplitudes in the adjacent far-red region. In the spectrum of the long-lived component, only a small negative band remains around the position of the ground-state absorption, but at the blue wing, the amplitude spectrum declines more steeply than the Pfr absorption band (cf. the inset in Figure 4b). This indicates that a positive absorption of the long-lived component is obviously overridden here by the strong ground-state bleaching.

To elucidate the role of proton transfer during the primary stages of the Pfr back conversion, experiments were carried out in which the protons of the chromophore and the apoprotein were replaced with deuterium ions. Table 1 compiles the time constants of the kinetic processes observed in deuterated Pfr. When compared to the results with nondeuterated Pfr, no significant differences indicative of a H−D isotope effect can be detected. The time constants remain nearly unchanged, irrespective of H−D exchange. Further, the amplitude spectra (not shown) are essentially the same for deuterated and nondeuterated Pfr.

Table 1 also shows the time constants determined in a 67% glycerol/buffer mixture. The most striking feature of these data is a significant lengthening of the shortest time constant (τ_1) from 560 fs in the aqueous buffer to 990 fs in the glycerol/buffer mixture. In contrast, the longer time constant (τ_2) remains approximately the same. Figure 5 compares the amplitude spectra of the two kinetic components in the aqueous and glycerol buffer. These spectra are nearly identical in the two solvents, except for a small red shift of ca. 10 nm in the spectrum of the 990 fs component

which is most likely due to an increase in the stimulated emission.

DISCUSSION

Pr to Pfr Phototransformation. The excited-state relaxation processes in the Pr → Pfr phototransformation have been studied intensively by several research groups in the past years. Our results presented here confirm previous findings by showing that three kinetic components are involved in the primary photoprocesses leading to the formation of the first photoproduct. On the basis of the global analysis of the time-resolved absorption difference spectra, the lifetimes associated with these components are 360 fs (τ_1), 1.8 ps (τ_2), and 34 ps (τ_3). The first photoproduct itself is seen as an additional comparatively long-lived component (τ_4), the lifetime of which is beyond the time resolution of our femtosecond measurements. However, our investigations are not restricted to a lifetime analysis but include the estimation of the amplitude spectra for the individual kinetic components, which allows for a more reliable interpretation of the kinetic mechanism underlying the primary events in the Pr photoconversion.

In this respect, the amplitude spectrum of the 34 ps component clearly reveals that this component can be assigned to the S_1-excited state of Pr. This follows from the spectral shape of the amplitude spectrum in the red and far-red region: (1) This spectrum is red-shifted by several nanometers from the ground-state absorption spectrum of Pr and (2) it closely matches the mirror-image type band displayed by the ground-state absorption spectrum. These spectral features indicate that the 34 ps component is mostly due to stimulated emission originating from the S_1-excited state of Pr.

According to our kinetic analysis, the 34 ps component is preceded by a fast 1.8 ps component (τ_2). On the basis of the amplitude spectrum, this component contributes to an excited-state absorption and ground-state depletion, suggesting that it is also due to excited-state Pr.

The question of whether the 1.8 ps component corresponds to the 5−15 ps component detected in earlier picosecond-resolved experiments arises (*16*, *17*, *19*, *20*). On one hand, it is possible that the time resolution reached in these experiments was not adequate to resolve the 1.8 ps lifetime. On the other hand, it is not impossible that the lifetime of this component is dependent on the excitation wavelength within the S_0-S_1 absorption as has been proposed previously (*17*, *19*). With the excitation at 610 nm in our experiments, the excited molecules have an excess vibrational energy of ∼1400 cm^{-1} which could be the reason for a substantial increase in the initial decay rate when compared with the excitation at longer wavelengths.

One could also argue that the 1.8 ps component results from nonlinear processes due to a two-photon excitation, i.e., from a high pump−pulse intensity or from an additional excitation caused by the chirp of the broadband white light continuum. However, for the following reasons, neither of these two assumptions is highly plausible. (1) We could show that the 1.8 ps kinetics do not change when the energy of the pump pulse is reduced to 60 and 30% of its initial value (5×10^{15} photons cm^{-2}). (2) We could not detect any absorption changes in experiments with a negative delay time, i.e., with the probe pulse preceding the pump pulse.

The amplitude spectrum of the long-lived component qualitatively resembles, in band position and relative amplitudes, the difference spectrum between lumi-R and Pr measured in absorption studies with nanosecond time resolution (*7*, *10*, *28*). This clearly indicates that the primary photoproduct observed under femtosecond excitation is identical to lumi-R. The appearance of lumi-R coincides with the 34 ps decay of the stimulated emission and excited-state absorption. It seems therefore very likely that lumi-R is directly populated from the S_1-excited state of Pr with a rise time of 34 ps.

The kinetics of the two fastest components, τ_1 and τ_2, are noticeably affected by solvent viscosity, while the component τ_3 does not change significantly. Although the latter component is related to the formation of lumi-R which should involve a substantial torsional motion around the C(15)═C(16) double bond of the Pr chromophore, it is not distinctly viscosity-dependent. The fact that the two fastest components τ_1 and τ_2 are influenced by solvent viscosity therefore suggests that coordinates associated with the surrounding protein matrix play a role in the initial excited-state motion out of the Franck−Condon state. Accordingly, the viscosity effect might reflect the hindrance of protein relaxational motions in the more viscous medium which obviously assist the relaxational processes in the chromophore.

Pfr to Pr Phototransformation. As could be shown from the kinetic analysis of the time-resolved absorption difference spectra, the primary processes in the Pfr → Pr phototransformation involve three kinetic components, one with a lifetime of 560 fs (τ_1), another with a lifetime of 3.8 ps (τ_2), and a third with a comparatively long lifetime (τ_3).

The amplitude spectrum of the fast 560 fs component reveals two main features: (1) The minimum of the bleaching band is slightly red-shifted from the stationary Pfr absorption spectrum, indicating that the negative amplitudes can be assigned to both ground-state depletion and stimulated emission. (2) The amplitude of this component predominates throughout the spectral region of the ground-state depletion and/or stimulated emission. It seems therefore likely that the 560 fs component corresponds to the S_1-excited state of Pfr.

The spectrum of the 3.8 ps component has strong negative amplitudes in the region where ground-state bleaching is observed and strong positive amplitudes at the red wing of the ground-state bleaching. As can be seen from this spectrum, the 3.8 ps component forms directly from the S_1-excited state. There is no indication of a stimulated emission in the spectrum. It therefore remains unclear whether this component represents an excited or a (hot) ground state. Irrespective of the electronic nature of this state, it precedes the formation of a comparatively long-lived state, the difference spectrum of which is given by the amplitude spectrum of the component τ_3. In this spectrum, only a small bleaching remains around the spectral position of the ground-state absorption. No positive absorption associated with this state is to be seen. But judging from the clear difference between the amplitude and the stationary absorption spectrum in the region of 600−720 nm, such an absorption is very likely masked by the strong ground-state bleaching. With respect to its negative band, the long time amplitude spectrum is similar to the difference absorption spectrum between lumi-F, the first photoproduct observed in time-resolved studies on the nanosecond time scale (*8*), and unphotolyzed Pfr.

From these facts, we propose that the long-lived component (τ_3) represents the first photoproduct on the path from Pfr to Pr. The photoproduct is similar to lumi-F with the exception that it exhibits a weaker absorption intensity in the red region. The reason for this effect could be that the chromophore is initially surrounded by still unrelaxed protein sites which subsequently undergo conformational relaxation, to give a relaxed lumi-F species with a well-developed red absorption band.

The replacement of protons in the Pfr chromophore and the protein moiety with deuterium ions does not affect the kinetics of the primary stages in the Pfr transformation. Neither the kinetic constants (Table 1) nor the amplitude spectra of the kinetic components are subject to a measurable isotope effect. This suggests that the primary steps in the Pfr phototransformation, including the formation of the first photoproduct, do not involve a rate-limiting proton-transfer reaction.

In contrast to deuteration, there is a striking effect of solvent viscosity on the primary relaxation processes. The depopulation kinetics of the primary excited state slow from 560 to 990 fs when the solvent viscosity is increased by the addition of 67% glycerol. This result suggests that the primary process in the Pfr transformation includes a molecular event that is hindered by increasing solvent viscosity. On the basis of FTIR studies, the Pfr → lumi-F transition involves the configurational isomerization at the C(15)═C(16) double bond of the chromophore (*12*, *14*). It appears therefore possible that the viscosity dependence of τ_1 reflects the double-bond isomerization of the Pfr chromophore in its primary photoprocess, or perhaps another torsional motion at the exocyclic methine bridges accompanying the isomerization process. This interpretation differs from that of the Pr forward reaction because the viscosity-dependent reaction step is associated with spectral changes in the amplitude spectra that might indicate an *E*,*Z* isomerization. However, at the present stage of our study, this argumentation does not definitely exclude the possibility that it is the conformational relaxation of an amino acid chain(s) near the chromophore which is prevented in a more viscous medium, similar to the situation in the Pr forward reaction.

A comparison of the primary processes in the photoconversion of Pr and Pfr indicates distinct differences in the kinetics of the two pathways. The kinetic processes occurring up to the formation of the first photoproducts are considerably faster in the Pfr → Pr photoreversion reaction than in the Pr → Pfr forward transformation. The reason for this could lie in different interactions of the Pr and Pfr chromophore with protein contact sites in the chromophore binding pocket. Thus, the Pfr chromophore may be in looser contact with the surrounding protein sites than the Pr chromophore and may therefore undergo configurational or conformational changes much faster. On the other hand, the difference in the reaction kinetics could also result from different electronic structures of the Pr and Pfr chromophore. More experimental evidence is required to support either one of these hypotheses.

ACKNOWLEDGMENT

We gratefully acknowledge the technical assistance of Mrs. M. Kläke.

REFERENCES

1. Furuya, M., and Song, P.-S. (1994) in *Photomorphogenesis in Plants* (Kendrick, R. E., and Kronenberg, G. M. H., Eds.) pp 105−140, Kluver Academic Publishers, Dordrecht, The Netherlands.
2. Quail, P. H., Boylan, M. T., Parks, B. M., Short, T. W., Xu, Y., and Wagner, D. (1995) *Science 268*, 675−680.
3. Quail, P. H. (1998) *Philos. Trans. R. Soc. London, Ser. B 353*, 1399−1403.
4. Thümmler, F., and Rüdiger, W. (1983) *Tetrahedron 39*, 1943−1951.
5. Rüdiger, W., Thümmler, F., Cmiel, E., and Schneider, S. (1983) *Proc. Natl. Acad. Sci. U.S.A. 80*, 6244−6248.
6. Linschitz, H., Kasche, V., Butler, W. L., and Siegelman, H. W. (1966) *J. Biol. Chem. 241*, 3395−3403.
7. Zhang, C.-F., Farrens, D. I., Björling, S. C., Song, P.-S., and Kliger, D. S. (1992) *J. Am. Chem. Soc. 114*, 4569−4580.
8. Chen, E., Lapko, V. N., Lewis, J. W., Song, P.-S., and Kliger, D. (1996) *Biochemistry 35*, 843−850.
9. Gensch, T., Churio, M. S., Braslavsky, S. E., and Schaffner, K. (1996) *Photochem. Photobiol. 63*, 719−725.
10. Schmidt, P., Gensch, T., Remberg, A., Gärtner, W., Braslavsky, S. E., and Schaffner, K. (1998) *Photochem. Photobiol. 68*, 754−761.
11. Mizutani, Y., Tokutomi, S., and Kitagawa, T. (1994) *Biochemistry 33*, 153−158.
12. Matysik, J., Hildebrandt, P., Schlamann, W., Braslavsky, S. E., and Schaffner, K. (1995) *Biochemistry 34*, 10497−10507.
13. Andel, F., III, Lagarias, J. C., and Mathies, R. A. (1996) *Biochemistry 35*, 15997−16008.
14. Foerstendorf, H., Mummert, E., Schäfer, E., Scheer, H., and Siebert, F. (1996) *Biochemistry 35*, 10793−10799.
15. Kneip, C., Hildebrandt, P., Schlamann, W., Braslavsky, S. E., Mark, F., and Schaffner, K. (1999) *Biochemistry 38*, 15185−15192.
16. Hermann, G., Lippitsch, M. E., Brunner, H., Aussenegg, F. R., and Müller, E. (1990) *Photochem. Photobiol. 52*, 13−18.
17. Holzwarth, A. R., Venuti, E., Braslavsky, S. E., and Schaffner, K. (1992) *Biochim. Biophys. Acta 1140*, 59−68.
18. Kandori, H., Yoshira, K., and Tokutomi, T. (1992) *J. Am. Chem. Soc. 114*, 10958−10959.
19. Savikhin, S., Wells, T., Song, P.-S., and Struve, W. S. (1993) *Biochemistry 32*, 7512−7518.
20. Teuchner, K., Schulz-Evers, M., Leupold, D., Strehlow, D., and Rüdiger, W. (1997) *Chem. Phys. Lett. 268*, 157−162.
21. Rentsch, S., Hermann, G., Bischoff, M., Strehlow, D., and Rentsch, M. (1997) *Photochem. Photobiol. 66*, 4399−4404.
22. Rentsch, S., Bischoff, M., Hermann, G., and Strehlow, D. (1998) *Appl. Phys. B 66*, 259−261.
23. Bischoff, M., Hermann, G., Rentsch, S., and Strehlow, D. (1998) *J. Phys. Chem. A 102*, 4399−4404.
24. Bischoff, M., Hermann, G., Rentsch, S., Strehlow, D., Winter, S., and Chosrowjan, H. (2000) *J. Phys. Chem. B 104*, 1810−1816.
25. Bischoff, M., Stobrawa, G., and Rentsch, S. (2000) *Laser Chem. 18*, 203−217.
26. Sarkar, H.-K., and Song, P.-S. (1981) *Biochemistry 20*, 4315−4320.
27. Kovalenko, S. A., Dabryakov, A. L., Ruthmann, J., and Ernsting, N. P. (1999) *Phys. Rev. A 59*, 2369−2384.
28. Ruzsicska, B. P., Braslavsky, S. E., and Schaffner, K. (1985) *Photochem. Photobiol. 41*, 681−688.
29. Brock, H., Ruzsicska, B. P., Arai, T., Schlamann, W., Holzwarth, A. R., Braslavsky, S. E., and Schaffner, K. (1987) *Biochemistry 26*, 1412−1417.

BI0011734